RSC Advances

PAPER

View Article Online
View Journal | View Issue

Cite this: *RSC Adv.*, 2026, **16**, 16622

Preparation and microwave absorption mechanism of cobalt ferrite/coal slime-based carbon composites

Liwei. Si, Jing. Gao,* Zhijun. Ma, Fuli. Liu and Maoyuan. Qian

Received 24th January 2026
Accepted 22nd February 2026

DOI: 10.1039/d6ra00652c

rsc.li/rsc-advances

Transforming low-ash coal slime into electromagnetic wave-absorbing materials can not only meet the growing demand for electromagnetic protection but also holds significant importance for promoting the transformation and upgrading of the coal industry. In this study, a series of cobalt ferrite/coal slime-based carbon composite absorbing materials were successfully prepared by loading cobalt ferrite nanoparticles onto a coal slime-based carbon substrate *via* a co-precipitation method. The results demonstrate that the composite exhibits optimal wave-absorption performance when the cobalt ferrite loading amount is 12.52 wt%. At a matching thickness of 3.5 mm, the minimum reflection loss reaches −32.08 dB at 12.73 GHz, with an effective absorption bandwidth as high as 8.84 GHz (covering 9.16–18.00 GHz). The microwave absorption mechanism of the composite is primarily attributed to magnetic loss induced by cobalt ferrite, including natural resonance and eddy current loss, as well as dielectric loss caused by coal slime-based carbon, involving interfacial polarization and dipole polarization. The effective combination of coal slime-based carbon and cobalt ferrite significantly optimizes the impedance matching characteristics of the composite. This research provides theoretical guidance for the high-value utilization of low-ash coal slime in the field of electromagnetic wave absorption.

1 Introduction

With the rapid development of modern electronic information technology and military stealth technology, electromagnetic waves provide convenience while also causing increasingly prominent problems of interference and pollution. Therefore, the development of efficient, lightweight, and broadband wave-absorbing materials holds significant strategic importance and application value for enhancing the stability of electronic devices, achieving stealth for military targets, and mitigating electromagnetic radiation pollution.[1] Among various types of wave-absorbing materials, ferrites have been widely studied as traditional magnetic absorbers due to their high saturation magnetization and excellent magnetic loss capabilities.[2,3] However, single ferrite materials often suffer from inherent drawbacks such as poor impedance matching, high density, and narrow absorption bandwidth, which limit their applications in lightweight and broadband absorption fields.[4] To overcome these limitations, compounding magnetic materials with dielectric loss materials, particularly constructing composite systems with carbon materials such as graphene, carbon nanotubes, and porous carbon, is considered an effective approach for optimizing impedance matching and achieving magneto-dielectric synergistic loss effects, thereby improving overall wave-absorption performance.[5,6]

On the other hand, promoting the efficient and high-value utilization of coal resources represents an important direction for sustainable development. The particles of coal slime are very fine, making it a high-quality material for preparing carbon sources. However, its current primary disposal method remains direct combustion for energy, which not only underestimates its carbon resource value but is also accompanied by emissions of greenhouse gases and pollutants.[7] Transforming low-ash coal slime from a traditional fuel into a precursor for high-performance carbon-based functional materials represents a potential breakthrough for realizing the resource utilization of coal slime and enhancing its added value. Carbon materials derived from coal-based carbon sources typically offer advantages such as low cost, tunable structures, and moderate conductivity, making them promising candidates as ideal dielectric components in wave-absorbing composites.[8,9]

Based on the above background, this study proposes the construction of a novel cobalt ferrite/coal slime-based carbon composite wave-absorbing material by loading magnetic cobalt ferrite nanoparticles onto a low-ash coal slime-based carbon substrate. On one hand, the tunable dielectric properties and lightweight porous structure of the coal slime-based carbon are utilized to improve the impedance matching of the composite system and reduce material density.[10] On the other hand, the strong magnetic loss provided by cobalt ferrite forms

School of Mining, Liaoning Technical University, Fuxin 123000, China. E-mail: jinggao1229@163.com

a synergistic mechanism with the dielectric loss of the carbon material, aiming to achieve excellent wave-absorbing performance characterized by light weight, strong absorption, and a broad frequency band.[11] This study not only provides a new approach for developing high-performance composite wave-absorbing materials but also opens up a promising new pathway for the high-value-added resource utilization of low-ash coal slime.

2 Experimental

2.1 Raw materials

The low-ash coal slime used in the experiment was sourced from a coal preparation plant in Xinjiang, China. After preliminary flotation de-ashing, the ash content of the obtained coal slime concentrate was 0.92%. The reagents used in the experiment included potassium hydroxide (KOH), cetyltrimethylammonium bromide ($C_{19}H_{42}BrN$), iron chloride hexahydrate ($FeCl_3 \cdot 6H_2O$), cobalt acetate tetrahydrate ($C_4H_6CoO_4 \cdot 6H_2O$), sodium hydroxide (NaOH), and anhydrous ethanol (CH_3CH_2OH). All chemicals were of analytical grade (AR) and supplied by Sinopharm Chemical Reagent Co., Ltd. The ultrapure water used in the experiment was prepared using a Milli–Q water purifier.

2.2 Preparation method

First, 2 g of coal slime and 4 g of KOH were placed in 15 mL of ultrapure water for ultrasonic dispersion. Then, they were treated in an oven at 100 °C for 20 hours. Subsequently, they were further processed in a microwave reactor operating at a frequency of 915 MHz for 25 minutes. After cooling, the product was washed and filtered to obtain coal slime-based carbon material.[12,13] The specific surface area of the carbon material is 1252 $m^2\ g^{-1}$, with a pore size distribution ranging from 0.4 to 0.7 nm, and a pore volume of 0.6831 $m^3\ g^{-1}$.

Cobalt acetate and iron chloride (with a molar ratio of cobalt to iron of 1 : 2) were placed in 80 mL of cetyltrimethylammonium bromide solution for ultrasonic dispersion. The pH of the reaction system was adjusted to 11 with sodium hydroxide and aged for 8 hours to obtain the precursor of cobalt ferrite. 2 g of coal slime-based carbon was placed in the cobalt ferrite precursor solution and crystallized in an autoclave at 180 °C for 8 hours to obtain cobalt ferrite/coal slime-based carbon composite material.[14,15] To investigate the effect of composition on performance, five composites with varying ratios of cobalt ferrite to coal slime-based carbon were prepared and labeled as C1, C2, C3, C4, and C5, respectively. A schematic illustration of the preparation process is shown in Fig. 1.

2.3 Testing and characterization

Phase analysis of the samples was performed using an Empyrean X-ray diffractometer (XRD) from Panalytical, Netherlands. The micro-morphology of the samples was observed using a JSM-7610F scanning electron microscope (SEM) and a JEM-2010 transmission electron microscope (TEM) from JEOL, Japan. Elemental composition and chemical state analysis were carried out with a K-alpha X-ray photoelectron spectrometer (XPS) from Thermo Scientific, USA. The complex permittivity (ε_r) and complex permeability (μ_r) of the samples in the frequency range of 1–18 GHz were measured using an HP8722ES vector network analyzer (VNA) from Agilent, USA, and the reflection loss (RL) was calculated based on eqn (1) and (2). Where Z_0 represents the impedance of free space. Z_{in} represents the input impedance. d represents the thickness of the absorber.[16,17]

$$RL(dB) = 20\ \log\left|\frac{Z_{in} - Z_0}{Z_{in} - Z_0}\right| \quad (1)$$

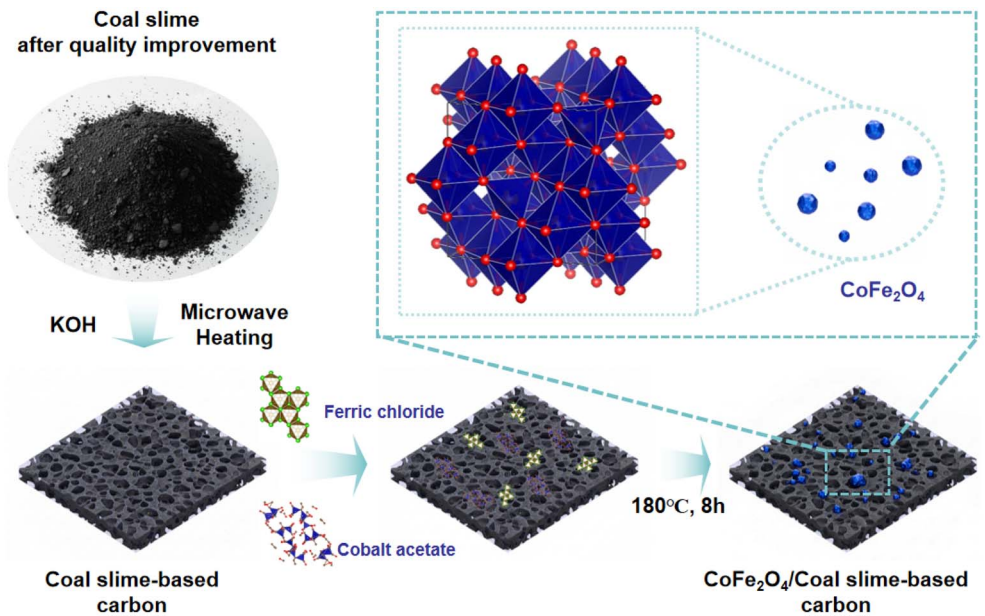

Fig. 1 Schematic diagram of the preparation process for the cobalt ferrite/coal slime-based carbon composite.

$$Z_{in} = Z_0\sqrt{\frac{\mu_r}{\varepsilon_r}}\tan h\left[j\frac{2\pi}{c}\sqrt{\mu_r\varepsilon_r}fd\right] \quad (2)$$

3 Results and discussion

3.1 The microstructure of cobalt ferrite/coal slime-based carbon

Fig. 2(a) displays the XRD patterns of the cobalt ferrite/coal slime-based carbon composites. In the patterns, the diffraction peaks of cobalt ferrite, as well as the diffuse peaks of amorphous carbon between 20–30°, can be observed. The quantitative results indicate that the ratio of cobalt ferrite to coal slime-based carbon can be controlled.[18]

Fig. 2(b–g) presents the SEM and TEM images of the C3 composite. The composite form of cobalt ferrite and coal slime-based carbon can be observed through Fig. 2(b). Fig. 2(c–e) show that the cobalt ferrite grains exhibit a size of approximately 25 nm, and energy-dispersive spectroscopy analysis did not detect any other impurity elements. The high-resolution TEM image (Fig. 2(f)) reveals lattice fringes with a spacing of 0.2961 nm, corresponding to the (220) crystal plane of cobalt ferrite. The continuous and parallel fringes suggest that the particle possesses a single-crystal structure. The selected-area electron diffraction (SAED) pattern (Fig. 2(g)) further confirms that the nanoparticles loaded on the coal slime-based carbon surface are cobalt ferrite.

Fig. 3 shows the XPS spectra of the cobalt ferrite/coal slime-based carbon composites. In the full survey spectrum (Fig. 3(a)), distinct peaks appear near binding energies of 284 eV, 529 eV, 710 eV, and 780 eV, corresponding to the characteristic signals of C 1s, O 1s, Fe 2p, and Co 2p, respectively.[19] Fig. 3(b) shows the high-resolution O 1s spectrum of the C3 composite, in which the three peaks located at 530.03 eV, 531.50 eV, and 533.10 eV can be assigned to lattice oxygen in the metal oxide, oxygen vacancies, and chemically adsorbed hydroxyl oxygen (O–H), respectively.[20,21] The fine spectrum of C 1s (Fig. 3(c)) reveals peaks at 284.76 eV, 285.84 eV, and 288.57 eV, corresponding to C–C, C–O–C, and O–C=O bonds, respectively.[22,23] These results demonstrate that the composite surface is rich in functional groups, which helps enhance the dissipation capability toward incident electromagnetic waves by inducing multiple relaxation mechanisms such as interfacial polarization and dipole polarization.[24]

3.2 The microwave absorption properties of cobalt ferrite/coal slime-based carbon

The RL of the cobalt ferrite/coal slime-based carbon composites was calculated according to eqn (1) and (2). Fig. 4 presents the reflection loss curves of the composites within the 1–18 GHz frequency range at different matching thicknesses, along with their corresponding effective absorption bandwidths (EAB, defined as the frequency width where RL ≤ −10 dB[25]). Sample C1 exhibited a minimum reflection loss (RL_{min}) of −23.49 dB at a frequency of 14.26 GHz, with an EAB coverage ranging from 10.69 to 18.00 GHz. Sample C2 exhibited an RL_{min} of −28.46 dB at a frequency of 14.26 GHz, with an EAB coverage ranging from 10.61 to 18.00 GHz. Sample C3 exhibited an RL_{min} of −32.08 dB at a frequency of 12.73 GHz, with an EAB coverage ranging from 9.16 to 18.00 GHz. Sample C4 exhibited an RL_{min} of −25.55 dB at a frequency of 11.88 GHz, with an EAB coverage ranging from 9.59 to 18.00 GHz. Sample C5 exhibited an RL_{min} of −19.67 dB at a frequency of 17.66 GHz, with an EAB coverage ranging from 12.05 to 18.00 GHz. The above results indicate that the ratio of cobalt ferrite to coal slime-based carbon in the composite material has a significant impact on its microwave absorption performance. It is particularly noteworthy that all samples exhibit relatively broad EABs, indicating the strong potential of this composite system for achieving broadband absorption.[26] Table 1 summarizes the RL and EAB of similar composite absorbing materials. It can be observed that the cobalt ferrite/coal slime-based carbon material in this work exhibits excellent performance.

3.3 The microwave absorption mechanism of cobalt ferrite/coal slime-based carbon

Fig. 5 displays the frequency-dependent curves of the complex permittivity ($\varepsilon_r = \varepsilon' - j\varepsilon''$), complex permeability ($\mu_r = \mu' - j\mu''$),

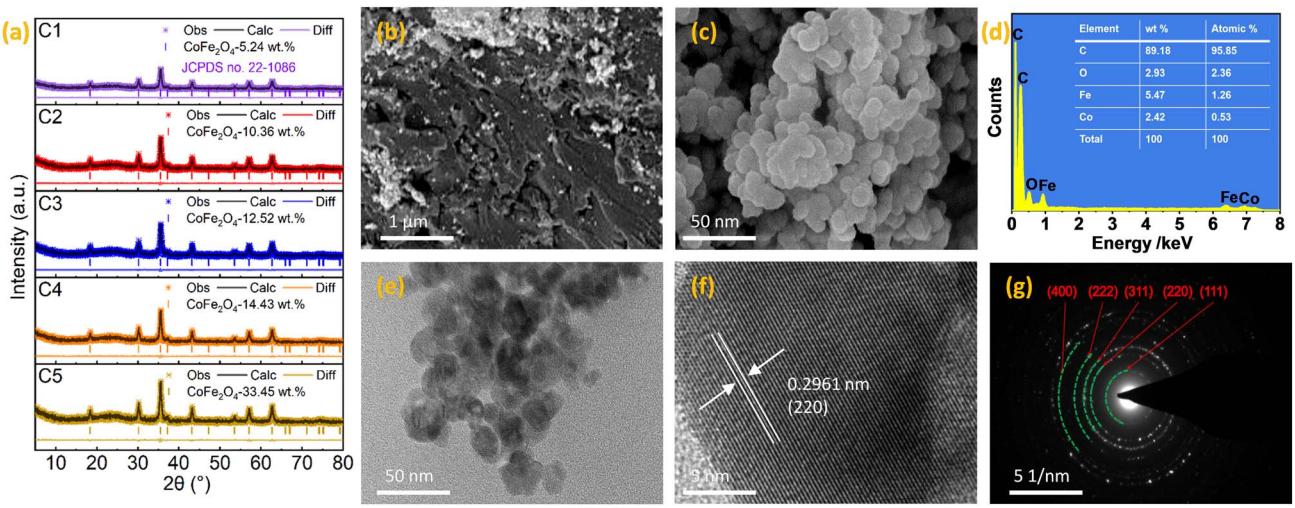

Fig. 2 (a) XRD patterns of samples C1–C5; (b–d) SEM-EDS images of sample C3; (e–g) TEM images of sample C3.

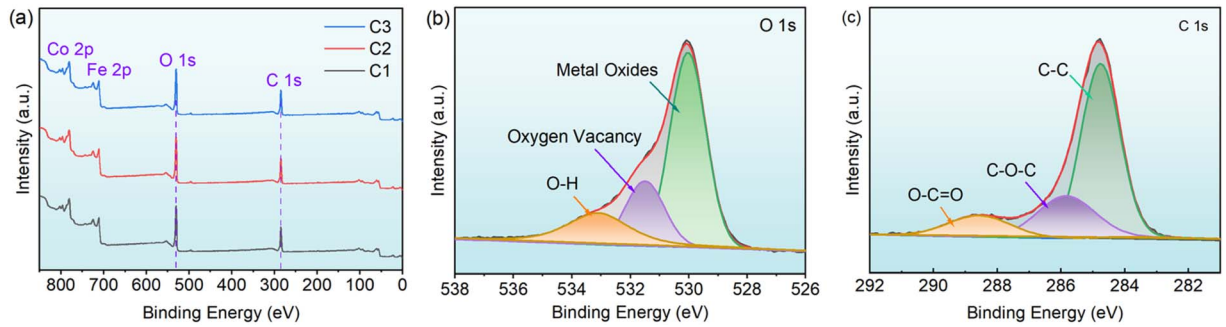

Fig. 3 XPS spectra of the cobalt ferrite/coal slime-based carbon composite. (a) Full survey spectrum; (b–c) fine spectra.

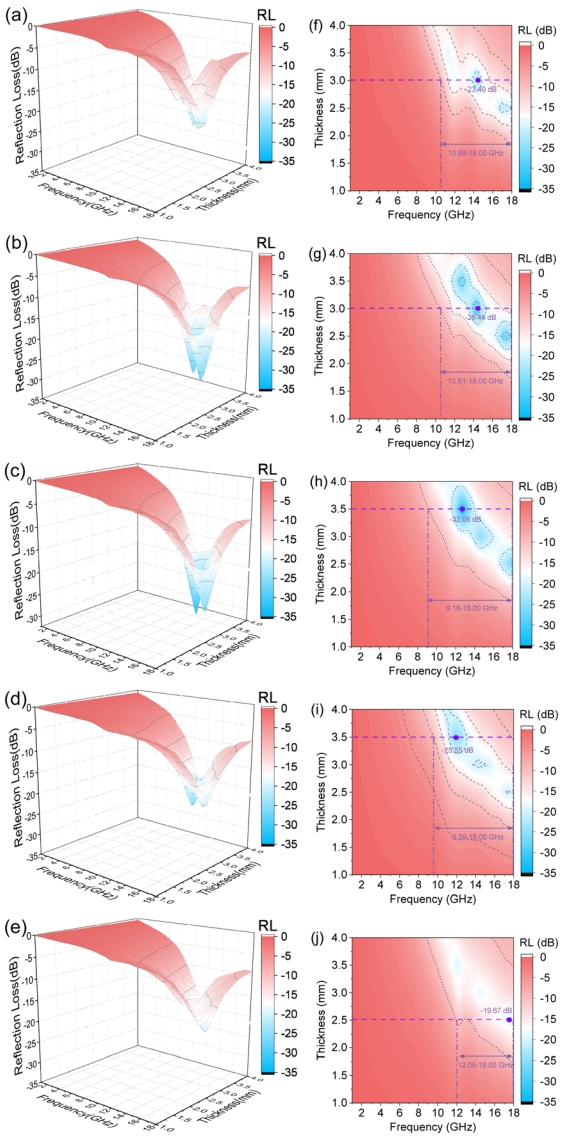

Fig. 4 RL (a–e) and EAB (f–j) curves of the cobalt ferrite/coal slime-based carbon composite (corresponding samples C1–C5) at different frequencies and thicknesses.

and the corresponding dielectric loss tangent ($\tan\delta_\varepsilon = \varepsilon''/\varepsilon'$) and magnetic loss tangent ($\tan\delta_\mu = \mu''/\mu'$) for the cobalt ferrite/coal slime-based carbon composites within the 1–18 GHz frequency range. The real and imaginary parts of the complex permittivity and complex permeability represent the material's capacity to store and dissipate electromagnetic energy, respectively.[31] As the compositional differences in the cobalt ferrite to coal slime-based carbon ratio among the five composites, and cobalt ferrite itself possesses both magnetic and dielectric loss characteristics, the real and imaginary parts of ε_r and μ_r for all samples do not vary linearly with frequency, as seen in Fig. 5(a–d), and their overall numerical ranges remain relatively limited.

Table 1 Performance comparison of similar composites

Samples	RL_{min} (dB)	EAB (GHz)	Ref.
$RGO/MWCNTS/ZnFe_2O_4$	−23.80	2.60	27
$Ni_{0.5}Co_{0.5}Fe_2O_4$@graphene	−30.92	0.61	28
$Co_{0.33}Ni_{0.33}Mn_{0.33}Fe_2O_4$/graphene	−24.29	8.48	29
$CoFe_2O_4/RGO/SiO_2$-epoxy	−24.80	4.50	30
$CoFe_2O_4$/coal slime-based carbon	−32.08	8.84	This work

As shown in Fig. 5(e), the C3 composite exhibits relatively higher tan δ_ε values, which aligns with the larger imaginary part of its complex permittivity (ε''), indicating stronger dielectric loss capability. Within the 1–18 GHz band, the dielectric loss of the composites primarily originates from multiple polarization mechanisms, including dipole polarization and interfacial polarization. The XPS results reveal that the coal slime-based carbon surface is rich in oxygen-containing functional groups, which can act as dipole centers and induce multiple dipole relaxation processes. Furthermore, according to the Maxwell–Wagner interfacial polarization theory, an increase in the number of heterogeneous interfaces enhances the interfacial polarization effect.[32] In this composite system, the numerous heterogeneous interfaces formed between cobalt ferrite and the coal slime-based carbon provide favorable conditions for interfacial polarization.

Fig. 5(f) shows that, except for the C1 sample with a lower cobalt ferrite content, the tan δ_μ values of other composite materials are relatively high, which is consistent with their characteristic of having a larger imaginary part of complex permeability (μ''), indicating that these samples exhibit strong magnetic loss capacity. Magnetic loss in absorbing materials typically includes hysteresis loss, eddy current loss, and residual loss.[33] Among these, eddy current loss is frequency-

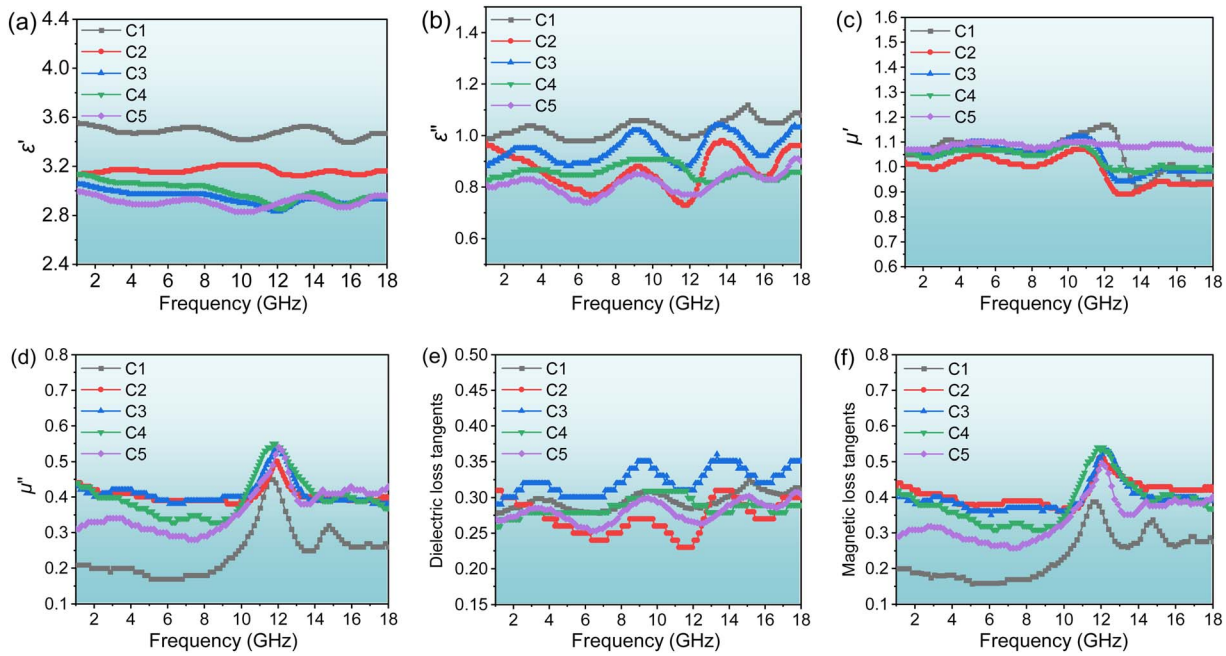

Fig. 5 Electromagnetic parameters of the cobalt ferrite/coal slime-based carbon composite. (a) ε', (b) ε'', (c) μ', (d) μ'', (e) tan δ_e, and (f) tan δ_m.

independent, while residual loss at high frequencies mainly stems from mechanisms such as natural resonance, domain wall resonance, and exchange resonance. Domain wall resonance generally occurs in the 1–100 MHz band.[34] To identify the dominant magnetic loss mechanism in this study, the eddy current loss coefficient C_0 ($C_0 = \mu''(\mu')^{-2}f^{-1} = 2\pi\mu_0 d^2\delta$ was calculated.[35] As shown in Fig. 7(a), the significant variation of the C_0 value within the 1–6 GHz band indicates that magnetic loss in this frequency range is primarily caused by natural resonance. In contrast, the C_0 value fluctuates less and stabilizes within the 6–18 GHz band, suggesting that eddy current loss dominates the magnetic loss in this region.[36]

In addition to sufficient attenuation capability, good impedance matching is another key factor determining wave absorption performance, which is governed by the material's complex permittivity and complex permeability. The degree of

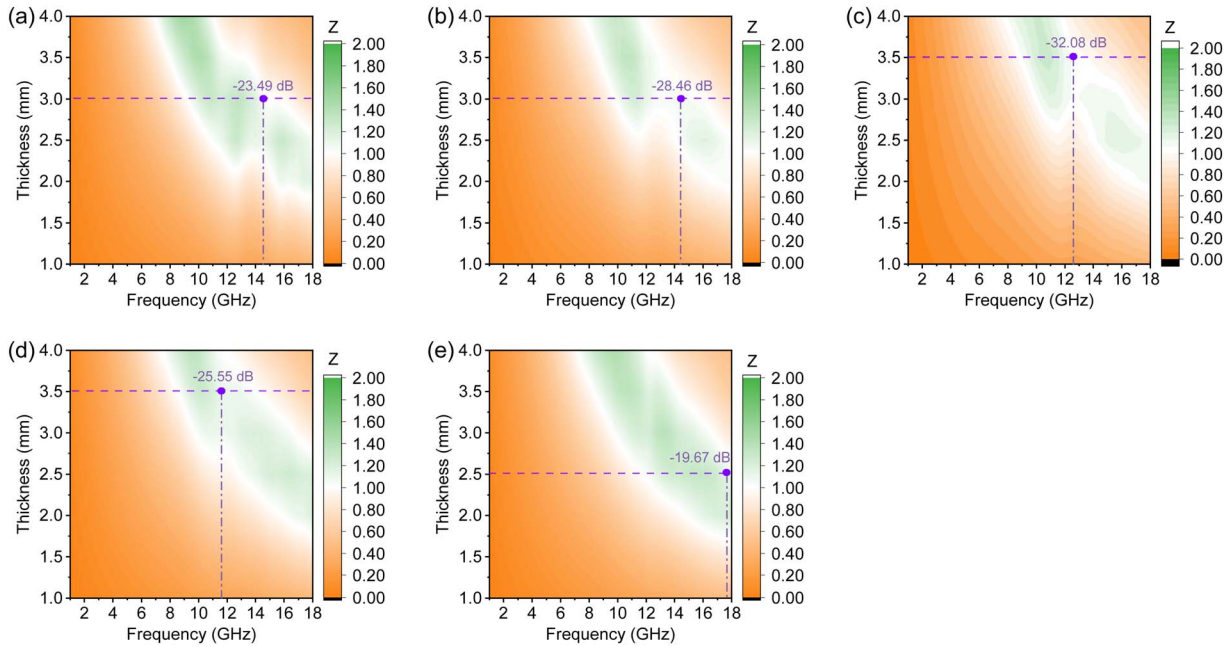

Fig. 6 Impedance matching diagram of the cobalt ferrite/coal slime-based carbon composite ((a–e) correspond to samples C1–C5 respectively).

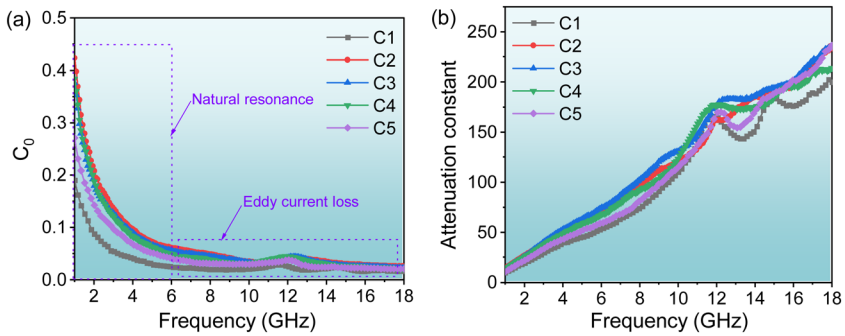

Fig. 7 (a) Magnetic loss C_0 values and (b) attenuation constant curves of the cobalt ferrite/coal slime-based carbon composite.

impedance matching can be characterized by the normalized input impedance modulus $|Z_{in}/Z_0|$ (eqn (3)); a value closer to 1 indicates that electromagnetic waves can more effectively enter the material interior with minimized surface reflection.[37] Fig. 6 shows the frequency distribution of $|Z_{in}/Z_0|$ for the five composites. At the optimal absorption frequency, the $|Z_{in}/Z_0|$ value for the C3 composite is 1.04, which is the closest to the ideal matching condition overall. This is one of the main reasons why the sample with this composition exhibits the optimal wave absorption performance. Furthermore, the attenuation constant α (eqn (4)) reflects the overall loss capability of electromagnetic waves within the material, with a larger α value representing stronger attenuation capability.[38] As shown in Fig. 7(b), the C3 composite possesses relatively higher α values across the entire frequency band, further confirming its excellent comprehensive wave absorption performance.

$$Z = \left|\frac{Z_{in}}{Z_0}\right| = \sqrt{\frac{\mu_r}{\varepsilon_r}}\tan h\left(j\frac{2\pi fd}{c}\sqrt{\mu_r\varepsilon_r}\right) \quad (3)$$

$$\alpha = \frac{\sqrt{2}\pi f}{c} \times \sqrt{(\mu''\varepsilon'' - \mu'\varepsilon') + \sqrt{(\mu''\varepsilon'' - \mu'\varepsilon')^2 + (\mu'\varepsilon'' + \mu''\varepsilon')^2}} \quad (4)$$

Based on the structural and compositional characteristics of the cobalt ferrite/coal slime-based carbon composites, their microwave absorption mechanism can be summarized as follows (illustrated in Fig. 8). Cobalt ferrite provides magnetic loss

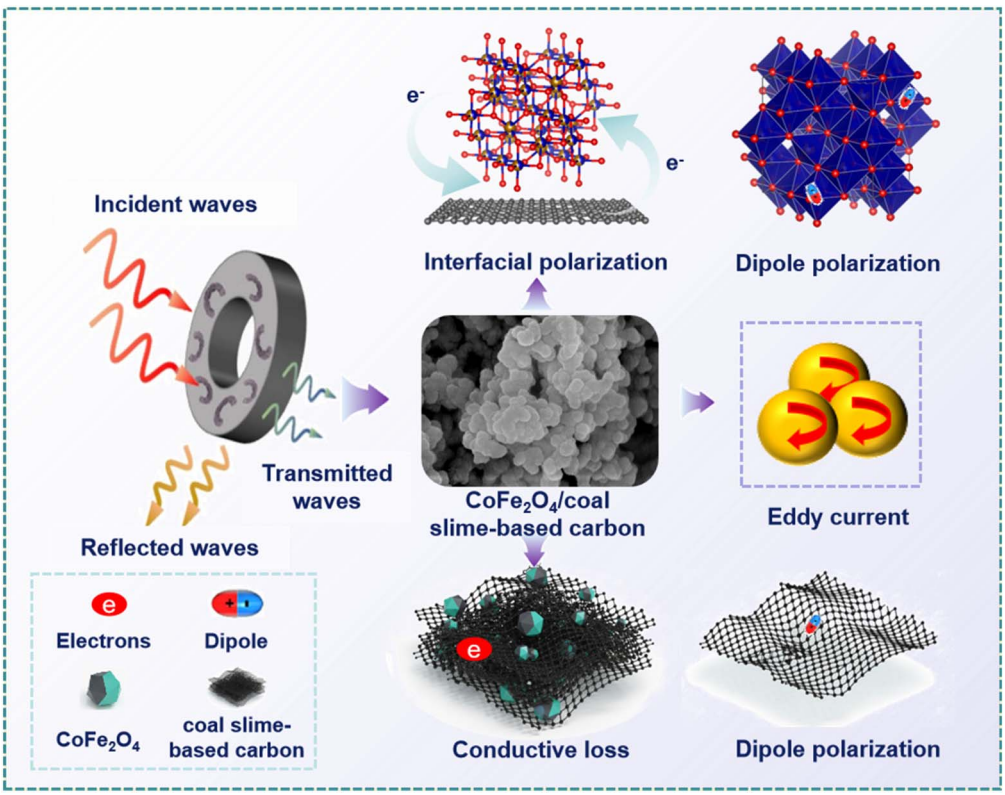

Fig. 8 Schematic diagram of the microwave absorption mechanism for the cobalt ferrite/coal slime-based carbon composite.

capability for composite materials, and its dense packing structure between particles intensifies the multiple scattering of incident electromagnetic waves. There are multiple heterogeneous interfaces between coal slime-based carbon and cobalt ferrite, and the dielectric loss and magnetic loss generated by the two are effectively adjusted to form good impedance matching.

In summary, the combination of the aforementioned multiple loss mechanisms and favorable impedance matching collectively contributes to the excellent microwave absorption performance of the cobalt ferrite/coal slime-based carbon composites, indicating that this material is a promising wave-absorbing system with good application prospects. In this study, cobalt ferrite was successfully loaded onto the surface of coal slime-based carbon material through a two-step hydrothermal reaction. The preparation process is simple, with minimal heat loss during the reaction and low energy consumption, which can serve as a reference for the synthesis of other similar composite materials. This preparation process is an ideal approach for the industrial preparation of microwave-absorbing materials.

4. Conclusions

In this study, cobalt ferrite/coal slime-based carbon composites were successfully prepared using low-ash coal slime-derived carbon as the matrix. The influence of the ratio between cobalt ferrite and coal slime-based carbon on the electromagnetic properties and microwave absorption performance was systematically investigated. The results indicate that when the cobalt ferrite loading amount is 12.52 wt%, the composite exhibits optimal wave-absorbing performance: at a matching thickness of 3.5 mm, a minimum reflection loss of −32.08 dB is achieved at 12.73 GHz, with an effective absorption bandwidth reaching 8.84 GHz, covering the frequency range of 9.16–18.00 GHz.

The microwave absorption mechanism of the composite was elucidated. First, cobalt ferrite contributes significant natural resonance and eddy current loss, endowing the material with strong magnetic loss capability. Second, the synergistic effect between cobalt ferrite and coal slime-based carbon effectively modulates the electromagnetic parameters of the composite system, achieving good impedance matching. Third, the closely packed structure formed by the cobalt ferrite particles promotes multiple scattering of electromagnetic waves. Fourth, abundant heterogeneous interfaces induce strong interfacial polarization relaxation, while the rich functional groups and structural defects on the surface of the coal slime-based carbon serve as dipole polarization centers, collectively enhancing the dielectric loss of electromagnetic energy.

Author contributions

Liwei Si: conceptualization, writing – original draft. Jing Gao: writing – review & editing. Zhijun Ma: methodology, investigation. Fuli Liu: review & supervision. Maoyuan Qian: review & validation.

Conflicts of interest

There are no conflicts to declare.

Data availability

All data supporting this study are available from the corresponding author upon reasonable request.

Acknowledgements

The authors would like to appreciate the financial support of the National Natural Science Foundation of China (52274265), the Liaoning Provincial Department of Science and Technology (20240338, 20240323), and the Liaoning Provincial Department of Education (LJ212510147040, JYTQN2023199). The authors extend their gratitude to Ms. Yunmeng Cao from Scientific Compass https://www.shiyanjia.com for providing invaluable assistance with the TEM analysis.

References

1 W. Fu, H. Wu, S. Liu, B. Chao, K. Deng and Y. Li, 3D-printed multi-material pyramids for broadband electromagnetic wave absorption, *Mater. Sci. Eng. B*, 2024, **307**, 117525.
2 Z.-X. Liu, H.-B. Yang, Z.-M. Han, W.-B. Sun, X.-X. Ge, J.-M. Huang, K.-P. Yang, D.-H. Li, Q.-F. Guan and S.-H. Yu, A Bioinspired Gradient Design Strategy for Cellulose-Based Electromagnetic Wave Absorbing Structural Materials, *Nano Lett.*, 2024, **24**, 881–889.
3 W. Shuai, H. Xia, C. Liang, C. Li and L. Zhang, A magnetic metal composite biomass carbon material with high efficiency and broadband wave absorbing property, *Biomass Convers. Biorefin.*, 2025, **15**, 6687–6698.
4 C. Ma, C. Zhang, M. Yuan, X. Guo, X. Liu, X. Zhang, C. Chai, Y. Zhang, H. Ma and Y. Wang, ZIF-67 derived CoNi@carbon/RGO composites with abundant heterogeneous interfaces for electromagnetic wave absorption, *Appl. Surf. Sci.*, 2024, **665**, 160283.
5 H. Xu, Y. Qi and Z. Zhang, The structure and microwave absorbing properties of PANI/BaFe 12 O 19 composites prepared by in-situ aniline polymerization method, *J. Alloys Compd.*, 2024, **1000**, 175079.
6 Z. Zhang, X. Yin, F. Zhang and Y. Chen, Surface morphology modulation and wave-absorbing properties of C@TiO2 composite microspheres, *J. Mater. Sci. Mater. Electron.*, 2024, **35**, 356.
7 P. Ling, M. E. Mostafa, K. Xu, C. Wang, H. Qing, Y. Jin, J. Xu, L. Jiang, Y. Wang, S. Su, S. Hu and J. Xiang, Co-combustion characteristics and reaction mechanism of coal slime and sewage sludge using a novel multilateral double volumetric parallel model and dendrite neural network, *J. Environ. Chem. Eng.*, 2024, **12**, 112058.
8 X. Zhu, X. Qian, M. Hao, Y. Zhang, Z. Zhang, S. Li and H. Wu, High performance electromagnetic wave absorbing material based on 3D flower-liked MXene, *J. Alloys Compd.*, 2024, **989**, 174440.

9 D. Lu, L. Wang, W. Dong, C. Chen, Z. Li, S. U. Rehman and H. Zou, MoS2 composite FeSiCr soft magnetic alloy materials and their wave-absorbing properties, *J. Alloys Compd.*, 2025, **1010**, 177835.
10 W. Zhang, X. Yang, Y. Wang, Y. Wang, X. Wu and Y. Shen, Fabrication of a tunable mesoporous polypyrrole/MXene composite with a sandwich structure for enhancing electromagnetic wave absorption performance, *RSC Adv.*, 2025, **15**, 10298–10309.
11 L. Du, Y. Li, Q. Zhou, J. Zhang, X. Wang, Y. Zhang, W. Cui, Z. Guo, H. Duan, C. Nan and X. Fan, Facile preparation of GNS/PyC@SiBCN aerogels with heterogeneous interfaces for broadband and tunable electromagnetic wave absorption, *Mater. Today Nano*, 2025, **29**, 100571.
12 Z. Ni, H. Bi, H. Shi, X. Liu, J. Tian, Y. Yao, L. He, K. Meng and Q. Lin, Effect of lignin on coal slime combustion characteristics and carbon dioxide emission, *J. Clean. Prod.*, 2024, **441**, 140884.
13 L. Si, J. Gao, Z. Ma, F. Liu and M. Qian, Multiphase interface and component synergism: electromagnetic wave absorption mechanism of Gd-doped cobalt ferrite/coal slime-based carbon composites, *Mater. Lett.*, 2026, **410**, 140265.
14 J. Gao, Z. Ma, F. Liu and X. Weng, Synthesis and electromagnetic wave absorption properties of Gd-Co ferrite@carbon core–shell structure composites, *Rare Met.*, 2023, **42**, 254–262.
15 J. Gao, Z. Ma, F. Liu, X. Weng and K. Meng, Preparation and microwave absorption properties of Gd–Co ferrite@silica@carbon multilayer core–shell structure composites, *Chem. Eng. J.*, 2022, **446**, 137157.
16 X. Ning, L. Yang, F. Rao, T. Wang, S. Wu and H. Huang, A novel electromagnetic wave absorption geopolymer originated from iron tailings and blast furnace slag, *Mater. Struct.*, 2025, **58**, 18.
17 J. Qian, D. Ma, X. Zhou, H. Liao, Q. Shan, S. Wang, Y. Wang and X. Zeng, Synthesis of SiOC@C ceramic nanospheres with tunable electromagnetic wave absorption performance, *J. Adv. Ceram.*, 2024, **13**, 1394–1408.
18 Z. Li, X. Chen, D. Liu, Y. Zhou, D. Pan and S. Shin, Recent advances in polymer-based composites for thermal management and electromagnetic wave absorption, *Adv. Compos. Hybrid Mater.*, 2025, **8**, 210.
19 H. Lu, C. Li, K. Chen, Q. He, F. Ren, J. Wu and R. Dai, Facile synthesis of $CoFe_2O_4$ @SiO_2 nanoparticles anchored on reduced graphene oxide for highly efficient electromagnetic wave absorption, *RSC Adv.*, 2025, **15**, 25872–25884.
20 Z. Jin, X. Feng, Y. Hou, H. Zhu and L. Wang, Lightweight and thermally insulating ZnO/SiCnw aerogel: A promising high temperature electromagnetic wave absorbing material with oxidation resistance, *Chem. Eng. J.*, 2024, **498**, 155110.
21 Q. Li, M. Ye and A. Han, Preparation and electromagnetic wave absorption properties of NiSe2@PANI composite material with cladding structure, *J. Mater. Sci.*, 2024, **59**, 16141–16157.
22 H. Wu, S. Deng, K. Deng, J. Jiang, S. Liu, B. Chao, S. Zeng, L. Gong and M. Liu, Enhanced SiC/NFG/Ni ternary composite microwave absorbing materials with micro-network structures produced by selective laser sintering, *Mater. Sci. Eng. B*, 2024, **310**, 117758.
23 Z. He, S. Zheng, Y. Shen, J. Tao, W. Xiong, S. Shu, X. Zeng and S. Song, Laser-induced layer-by-layer removal and thermo-mechanical action mechanisms of FeCo-based multilayer wave-absorbing coatings, *J. Mater. Sci. Technol.*, 2024, **190**, 10–23.
24 F. Gu, W. Wang, H. Meng, Y. Liu, L. Zhuang, H. Yu and Y. Chu, Lattice distortion boosted exceptional electromagnetic wave absorption in high-entropy diborides, *Matter*, 2025, **8**, 102004.
25 H. Xu, M. Liu, L. Huang, X. Zhang, Z. Ma, C. Zhu, F. Cao and Y. Chen, Enhanced dielectric loss via six-coordinated Er single atoms on porous carbon nanofibers for high-performance electromagnetic wave absorption, *Adv. Funct. Mater.*, 2025, **35**, 2502952.
26 J. Liu, B. Cui and B. Pang, Preparation and Properties of Magnesium Oxysulfide Cement Based Foam Board Absorbing Material, *J. Wuhan Univ. Technol., Mater. Sci. Ed.*, 2024, **39**, 118–125.
27 R. Shu, W. Li, X. Zhou, D. Tian, G. Zhang, Y. Gan, J. Shi and J. He, Facile preparation and microwave absorption properties of RGO/MWCNTs/ZnFe2O4 hybrid nanocomposites, *J. Alloys Compd.*, 2018, **743**, 163–174.
28 P. Yin, Y. Deng, L. Zhang, W. Wu, J. Wang, X. Feng, X. Sun, H. Li and Y. Tao, One-step hydrothermal synthesis and enhanced microwave absorption properties of Ni0.5Co0.5Fe2O4/graphene composites in low frequency band, *Ceram. Int.*, 2018, **44**, 20896–20905.
29 J. Peng, Z. Peng, Z. Zhu, R. Augustine, M. M. Mahmoud, H. Tang, M. Rao, Y. Zhang, G. Li and T. Jiang, Achieving ultra-high electromagnetic wave absorption by anchoring Co0.33Ni0.33Mn0.33Fe2O4 nanoparticles on graphene sheets using microwave-assisted polyol method, *Ceram. Int.*, 2018, **44**, 21015–21026.
30 R. Jaiswal, K. Agarwal, V. Pratap, A. Soni, S. Kumar, K. Mukhopadhyay and N. Eswara Prasad, Microwave-assisted preparation of magnetic ternary core-shell nanofiller (CoFe2O4/rGO/SiO2) and their epoxy nanocomposite for microwave absorption properties, *Mater. Sci. Eng., B*, 2020, **262**, 114711.
31 Y. Dou, X. Zhang, X. Zhao, X. Li, X. Jiang, X. Yan and L. Yu, N, O-Doped Walnut-Like Porous Carbon Composite Microspheres Loaded with Fe/Co Nanoparticles for Adjustable Electromagnetic Wave Absorption, *Small*, 2024, **20**, 2308585.
32 W. Wang, L. Wang, L. Wang, G. Liu, C. Ge, K. Xu, W. Wang and L. Hu, Research Progress of Absorbing Metamaterials Based on Different Material Systems, *Rare Met. Mater. Eng.*, 2024, **53**, 856–869.
33 D. Xiang, Q. He, D. Lan, Y. Wang and X. Yin, Regulating the phase composition and microstructure of Fe3Si/SiC nanofiber composites to enhance electromagnetic wave absorption, *Chem. Eng. J.*, 2024, **498**, 155406.

34 C. Ma, S. Xie, Z. Wu, Z. Ji and J. Wang, Research and simulation of electromagnetic wave absorbing performance for lightweight cement-based materials containing expanded polystyrene with different particle sizes and carbon black, *Constr. Build. Mater.*, 2024, **430**, 136496.

35 N. Kaushik, P. Singh, S. Rana, N. G. Sahoo, F. Ahmad and M. Jamil, Self-healable electromagnetic wave absorbing/shielding materials for stealth technology: Current trends and new frontiers, *Mater. Today Sustain.*, 2024, **27**, 100828.

36 D. D. Lim, J. Lee, J. Park, J. Lee, D. Noh, S. Park, G. X. Gu and W. Choi, Multifunctional seamless meta-sandwich composite as lightweight, load-bearing, and broadband-electromagnetic-wave-absorbing structure, *Addit. Manuf.*, 2024, **95**, 104515.

37 H. Zhang, C. Liu, Q. Zhang, T. Lu, Z. Huang, N. Li and C. Ma, The effects of phase interfaces in SmFeN/YSZ composite thermal barrier materials on electromagnetic wave-absorbing properties, *Ceram. Int.*, 2024, **50**, 27586–27595.

38 R. Lin, X. Li, Q. Fan, S. Zhang and W. Wang, Wave-absorbing material-assisted microwave freeze-drying of initially unsaturated coffee frozen material: Numerical simulation and experimental verification, *Chem. Phys. Lett.*, 2024, **838**, 141090.